UNIVERSIDAD REGIONAL AMAZÓNICA IKIAM

Facultad de Ciencias de la Tierra y Agua

Ingeniería en Geociencias

Tomografía sísmica en la caracterización de la mega-falla Puná-Pallatanga-Cosanga-Chingual

Diana Liced Quilumba Dutan

27 de abril de 2021, ciudad de Tena, Napo, Ecuador

Declaración de derecho de autor, autenticidad y responsabilidad

Tena, 27 de abril de 2021

Yo, Diana Liced Quilumba Dutan con documento de identidad N° 1725114977, declaro que los resultados obtenidos en la investigación que presento en este documento final, previo a la obtención del título "Tomografía Sísmica en la caracterización de la mega-falla Puná-Pallatanga-Cosanga-Chingual" son absolutamente inéditos, originales, auténticos y personales.

En virtud de lo cual, el contenido, criterios, opiniones, resultados, análisis, interpretaciones, conclusiones, recomendaciones y todos los demás aspectos vertidos en la presente investigación son de mi autoría y de mi absoluta responsabilidad.

Por la favorable atención a la presente, suscribo de usted,

Atentamente,

Firma:

_____

Diana Liced Quilumba Dutan

INVESTIGACIÓN | Parroquia Muyuna, kilómetro 7 vía a Alto Tena
INNOVACIÓN | Tena · Napo · Ecuador
EDUCACIÓN | Telf.: (06) 370 0040 · (06) 299 9160

www.ikiam.edu.ec
@u_ikiam IkiamOficial u_ikiam Universidad Ikiam

ii
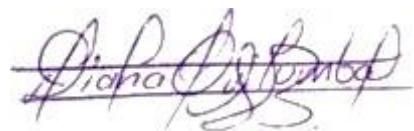
Certificado de dirección de trabajo de integración curricular

Certifico que el trabajo de integración curricular titulado: Título: "Tomografía Sísmica en la caracterización de la mega-falla Puná-Pallatanga-Cosanga-Chingual", en la modalidad de: proyecto de investigación en formato artículo original, fue realizado por: DIANA LICED QUILUMBA DUTAN, bajo mi dirección.

El mismo ha sido revisado en su totalidad y analizado por la herramienta de verificación de similitud de contenido; por lo tanto, cumple con los requisitos teóricos, científicos, técnicos, metodológicos y legales establecidos por la Universidad Regional Amazónica Ikiam, para su entrega y defensa.

Tena, 22 de abril de 2021

Firma:

Firmado electrónicamente por:
**JOSE
SEBASTIAN
ARAUJO SORIA**

……………………………

José Sebastián Araujo Soria, PhD.
C.I: 1802672871

INVESTIGACIÓN | Parroquia Muyuna, kilómetro 7 vía a Alto Tena
INNOVACIÓN | Tena · Napo · Ecuador
EDUCACIÓN | **Telf.:** (06) 370 0040 · (06) 299 9160

www.ikiam.edu.ec
@u_ikiam   IkiamOficial   u_ikiam   Universidad Ikiam

iii

AGRADECIMIENTOS

Me permito expresar mi profundo agradecimiento;

A PhD. Sebastián Araujo, por su disposición a guiar el presente trabajo de investigación, por su paciencia, sus observaciones y recomendaciones. Su apoyo fue fundamental para el desarrollo de este estudio.

Al Grupo de Investigación en Geofísica y Geotecnia dentro del cual está incluido este proyecto de investigación.

Al laboratorio Calcul Intensif / Modélisation / Expérimentation Numérique et Technologique CIMENT de la Universidad Grenoble Alpes, Francia, por su auspicio a este proyecto de investigación.

A los docentes de la carrera de Ingeniería en Geociencias, quienes durante estos años han compartido sus conocimientos, experiencias y enseñanzas. Su dedicación han sido clave en la formación de tantos futuros profesionales de Ciencias de la Tierra, entre los cuales me incluyo.

DEDICATORIA

A mi familia, quienes han estado siempre a mi lado celebrando mis logros y levantándome en mis caídas.

A mi madre, por creer y confiar en mí, por su esfuerzo y su infinito amor. Y por darme el mayor regalo, la vida.

A mis hermanas, Johanna y Verónica quienes han sido ejemplo de perseverancia, han sido mi apoyo en cada momento y han marcado el camino para llegar a donde estoy hoy en día.

A mis hermanos, Vinicio, Jorge Luis y Carlos, quienes, con su naturalidad yespontaneidad han llenado mis días de inmensa alegría y me han enseñado que cuandohaces lo que amas, no importa el cansancio o las dificultades, tu corazón siempre estarálleno.

A mis amigos, Andrea y Jimmy por ser la mejor compañía durante estos años de universidad, por cada momento, por cada risa, por las extensas charlas y por todos los momentos que aún nos quedan por construir.

A Nicholas y Michael por ser amigos y mentores y al resto del equipo YAKUM, por sus enseñanzas y por confiar en mis capacidades. Por ser mi inspiración y por demostrarme que el trabajo que se hace con amor crece grande y fuerte como los ceibos centenarios en la selva.

Gracias a todos y todas por ser luz.

ÍNDICE GENERAL

ÍNDICE DE FIGURAS

segmento Cosanga (superior derecha) usando la variación de la onda P (%). El movimiento en masa del Río Bermejo indicado con un círculo rojo se ubica en el contacto entre las fallas. **Pág. 18**.

6. Sección tomográfica del segmento Chingual. El mapa muestra el centro de las cajas tomográficas (puntos rojos) y su extensión E-W (líneas naranja). Los segmentos de Chingual se indican en el mapa (líneas azules punteadas). Las secciones tomográficas se modelaron usando el parámetro de variación de la velocidad de la onda P, dado en porcentaje (ΔVp). (h) cerca del poblado La Sofia, y

(i) cerca del poblado La Bonita. Las secciones tomográficas se orientan N90°E. Los puntos negros indican los eventos registrados por RENSIG hasta 2016. **Pág. 20**.

7. Secciones tomográficas de la CCPP. El modelo tomográfico representa la variación de la velocidad de la onda P, medida en %. Segmento Puná (J) orientado N148°E, segmento Pallatanga (K) orientado N121°E, segmento Cosanga (L) orientado N110°E y segmento Chingual (M) orientado N127°E. El rectángulo blanco indica loseventos sísmicos considerados para inferir la profundidad y ancho de las trazas de falla. La parte inferior izquierda muestra los ángulos de buzamiento de cada segmento. **Pág. 23.**

ÍNDICE DE TABLAS

RESUMEN

La subducción de la placa oceánica de Nazca bajo la placa Sudamericana y la oblicuidad de esta subducción ha generado el movimiento NE de la Astilla Norandina (NAS) cuyo límite oriental en Ecuador es la mega-falla Chingual-Cosanga-Pallatanga- Puná (CCPP). La CCPP es un sistema de fallas rumbo-deslizantes y sus segmentos representan algunas de las estructuras sísmicas intra-continentales más activas en Ecuador. Este estudio proporciona las primeras imágenes tomográficas de la corteza a lo largo de la CCPP para contribuir en la caracterización de su geometría. Para ello, se utilizarán datos sísmicos, modelos de velocidad de ondas sísmicas, mapas topográficos y geológicos. Las características geométricas de los segmentos de falla se obtuvieron mediante tomografía de tiempo de viaje.

La tomografía de los segmentos Puná y Chingual muestra ángulos de buzamiento casi verticales. La sección sur de Pallatanga muestra un ángulo de inmersión de 75 ° orientado hacia el oeste y aumenta un buzamiento casi vertical hacia el norte. El segmento Cosanga es el único segmento inverso de la CCPP. La convergencia de dos fallas que componen este segmento podría relacionarse con el deslizamiento superficial del Río Bermejo. El segmento Chingual avanza N-NE y marca la separación entre litologías sedimentarias y metamórficas. Esta investigación presenta imágenes de la corteza en profundidad para la megafalla CCPP y las asociaciones con la litología de sus segmentos para ofrecer una interpretación completa de la geometría y sismicidad de este sistema de fallas.

Palabras clave: tomografía sísmica, actividad sísmica, CCPP, falla rumbo- deslizante, falla inversa, eventos sísmicos.

ABSTRACT

Subduction of the Nazca oceanic plate under the South American plate and the obliquity of this subduction has generated the NE movement of the Astilla Norandina (NAS) whose eastern limit in Ecuador is the Chingual-Cosanga-Pallatanga-Puná mega- fault (CCPP). The CCPP is a strike-slip fault system and its segments represent some of the most active intra-continental seismic structures in Ecuador. This study provides the first tomographic images of the cortex along the CCPP to contribute to the characterization of its geometry. In order to achieve this objective, seismic data, seismic

wave velocity models, topographic and geological maps were used. The geometric characteristics of the fault segments were obtained by travel-time tomography. Tomography of the Puná and Chingual segments shows almost vertical dipping angles. The southern section of Pallatanga shows a dipping angle of 75 ° oriented to the west and increases to a near vertical dip to the north. The Cosanga segment is the only reverse segment of the CCPP. The convergence of two faults that make up this segment could be related to the superficial landslide of the Bermejo River. The Chingual segment advances N-NE and marks the separation between sedimentary and metamorphic lithologies. This investigation presents images of the crust in depth for the CCPP mega-fault and the associations with the lithology of its segments to offer a complete interpretation of the geometry and seismicity of this fault system.

Keywords: seismic tomography, seismic activity, CCPP, strike-slip fault, reverse fault, seismic events.

Seismic Tomography in the characterization of Puná-Pallatanga-Cosanga-Chingual mega-fault

INTRODUCTION

Ecuador is located in the subduction zone of the Nazca Plate and the South American plate. This subduction dynamics are estimated to happen since the Lower Jurassic at approximately 190Ma. This oceanic plate subduction beneath the continental lithosphere produces intense intracontinental geological deformation, volcanism, and high-magnitude earthquakes along the subduction margin (Bilek, 2010; Lonsdale, 1978).In addition, the eastward motion of a large block in northern South America, known as the North Andean Sliver (NAS), and several local fault complexes constitute geotectonicfactors that generate great seismic activity (Nocquet et al., 2014).

Fault complexes in the country have been extensively studied; Alvarado et al., (2016) describe the major fault systems and their sense of motion; one of those active fault systems is the Chingual-Cosanga-Pallatanga-Puná (CCPP) mega fault. The existenceof this mega-fault and its dynamics of movement surround the NAS kinematic behavior.Their study describes the CCPP mega-fault (Figure 1) as the eastern boundary of the NAS. This continuous fault system corresponds to dextral strike slip and reverse segments with an SW-NEdirection.

Several studies focused on the geodynamic aspect of Ecuador have been carried out. One of the studies developed by Nocquet et al., (2014) described the NAS movementby using geodetic data to quantify the Northern Andes deformation showing that NAS motion occurs parallel to the subduction zone and is controlled by the obliquity characteristics of the subduction of plates. Similarly, its movement is linked to several geomorphological

features observed in the continent, one of them is the CCPP.

Regarding the CCPP, Baize et al., (2015) establish that the Pallatanga segment would extend north of Rumipamba in the Riobamba basin, dividing into an NNE-SSW group to N – S and another group of NE-SW segments. Whilst, Witt et al., (2005) establishes that the Gulf of Guayaquil's development is associated with the Northeast movement of the NAS, and its evolution is associated with the fault system made up of Puná and Santa Clara segments. The Cosanga and Chingual segments are identified in few investigations focused on seismicity and cortical deformation (Eguez et al., 2003; Yepes et al., 2016), but they do not have in-depth investigations.

In reference to the seismicity studies carried out, several reports published by the Instituto Geofísico (IG) of the Escuela Politécnica Nacional have been possible thanks to the Red Nacional de Sismómetros del IG (RENSIG), in operation since the 80s. Since then, records of seismic events that occur in Ecuador can be obtained.

However, many of the most important seismic events in Ecuador occurred before RENSIG started up. Those that occurred along CCPP are described in table 1.

Table 1. Historical earthquakes in Ecuador associated with the cortical seismic activity of the segments of the mega-fault CCPP. Modified from: (Beauval et al., 2013).

Locality/ Year	Associated fault system	Magnitude(Mw)
Chimborazo / 1645	Pallatanga	6.7 – 7.3
Chimborazo / 1786	Pallatanga	5.4 – 6.2
Chimborazo / 1797	Pallatanga	7.1
Napo / 1987	Cosanga	6.9

The location of these earthquakes corresponds to an indirect geophysical method. (Araujo

et al., 2009) carried out a double-difference tomography for the Pisayambo seismic nest, owing to that it is possible to improve the precision of the location of hypocenters of the seismic events in this area. Similarly, Araujo, (2016) implemented the travel time seismic tomography method for RENSIG data nationwide. This last work sets the basis for the development of the present study.

The development of this research focuses on generating tomographic images of the segments of the CCPP fault to describe its geometry and associate it with an interpretation of seismicity based on relocated seismic records in the study area and its geomorphic surface features. We use the software INSIGHT to solve the joint inversion of velocity models and earthquake hypocenters. Previous uses of INSIGHT define splay faults in subduction zones in Chile (Pastén-Araya et al., 2021) and detail tectonic faults and geological formations in the Ecuadorian Andes (Paredes & Araujo, 2021).

Identifying the study area's geometry characteristics could help redefine or improve the studies and maps of seismic hazard that are delivered to the population and for use as a source to establish management strategies for possible seismic events.
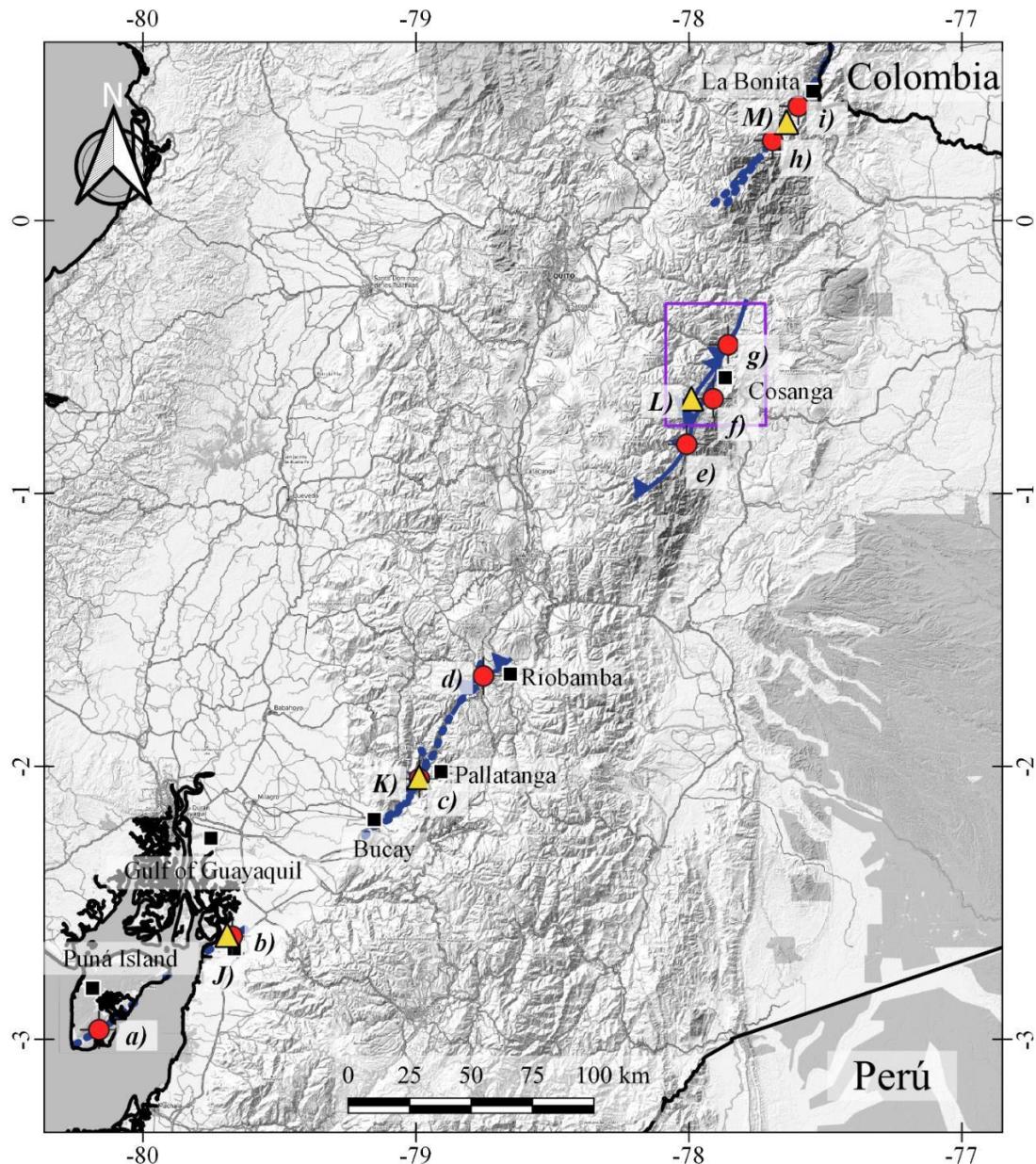
Figure 1. Location of tomographic cross-sections with azimuth N90°E (red dots) along with CCPP fault segments. Tomographic cross-sections perpendicular to the fault trace (yellow triangles). Letters indicate the cross-section in figures 2, 3, 4 and 6. Quaternary

faults (bluelines) from (Egüez et al., 2003; Alvarado, 2009). Cosanga segment horizontal

tomographic box analysis (violet rectangle, Figure 5).

SRUCTURAL CONTEXT OF CCPP

CCPP is composed of four main segments which correspond to four fault systems: Chingual, Cosanga, Pallatanga and Puná. These four structures represent the major tectonic system in Ecuador (Alvarado, 2012) and their slip rate has been determined in several studies to be among 7 - 8 mm/yr (Alvarado, 2012; Nocquet et al, 2014; Baize et al, 2014; Alvarado et al, 2016; Beauval et al, 2018). The CCPP is composed mainly of dextral strike-slip faults and one reverse component, Cosanga Fault System. The following sections exposes the structural characteristics of each segment compiled from previous work presented by different authors.

Puná Fault System

Puná segment is a strike-slip fault type with dextral component (Egüez et al, 2003). This fault system can be traced from Santa Clara Island, through Puná Island until it reaches the Gulf of Guayaquil (Dumont et al, 2005). Egüez et al (2003) and Dumont et al (2005) describe the southeastern section of Puná island where the Zambapala ridge is crosscut NE by the Puná Fault marking the limit between two sedimentary formations Tablazo Formation and Puná Formation. It comprises active faults such as the Zambapala flower structure, the Santa Clara Fault and the Gulf of Guayaquil flower structure, which is corresponds to the offshore extension of Puna-Pallatanga system (Alvarado et al, 2016). Puná segment shows marine terraces lifted up during interglacial periods. Northern Puná Island consist of marine deposit sediments. To the Southeast of Puná two ridges Zambapala and San Ramon elevate over 170 m.a.s.l., and on top a pull-apart basin has formed due to transpressional efforts. (Dumont et al, 2015).

Parameters for the Puná Fault geometry is given by Egüez et al, (2003) where authors provide a fault length of 49 Km and an average strike N46°E. Beauval et al, (2018) develop a geologic model to estimate seismic hazard and they provide a 172 Km length for this segment, as well as a maximum depth and width of 18 Km. Dip is reported to be vertical whilst slip rate reportedby Dumont et al, (2005) is between the range of 5.8 – 8 mm/yr after corroborated with GPS data by Alvarado et al, (2016) presenting a value of 7.1 mm/yr.

Pallatanga Fault System

Pallatanga has been extensively studied. It extends about 200Km NE from Gulf of Guayaquil, crosscuts the Western Cordillera and separates into segments, Southern segment connects to Puna Fault System and extends from east of Gulf of Guayaquil to Pallatanga, entering the Western Cordillera transpressional efforts have given rise to Cutuguay uplift. Center section extensively described by Alvarado et al 2016 runs from Bucay to Rumipamba town and the northern section of the fault extends near the city of Riobamba. Other segments might be markingthe transition between the latter segment and the Cosanga Fault System Alvarado et al (2016), at the Pisayambo nest, one of the most seismic zones in Ecuador Araujo et al (2017). According to Egüez et al (2003).

Pallatanga northern section presents an average strike of N28°E and dip of 75°W. Central section describes a N16°E strike whilst southern section has a N18°E strike. Depth and width are assigned values of 18 and 19 Km, respectively (Beauval et al, 2018).

Baize et al (2014) propose a slip rate to be 2.5 – 4.6 mm/yr. Again, Baize et al, 2020 infer slip rates for central and southern sections to be 2 to 6 mm/yr, respectively. Alvarado, (2012) describe morphologic characteristics for this segment such as lateral displacement of rivers and hills, scarps, benches, sag ponds, etc.

Cosanga Fault System

Cosanga Segment correspond to an ancient tectonic system active during the Jurassic, it

marks a limit between metamorphic rocks of the Cordillera Real and the non-deformed domains of the Sub-Andean Zone. This segment extends almost N-S through the Rio Cosanga valley to connect to the Rio Quijos valley (Alvarado et al, 2016). It also shows compressive component started in the Quaternary. It is mainly reverse fault with a secondary dextral component (Alvarado, 2012).

Beauval et al, (2018) consider a 189 Km trace for this segment. Average strike reported by Egüez et al, (2003) is N28°E. Depth and width are reported to be 25 and 36 Km (Beauval et al, 2018). According to Egüez et al (2003), the fault dips to the northwest, dipping angle remains unknown. Beauval et al, 2018 assigns it a dipping angle of 40°. The northern section of the Cosanga fault system shows reverse faults dipping ∼70° to the west (Tibaldi et al, 2007). Slip rate reported by Beauval et al, (2018) is 9.0 mm/yr.

The main geomorphic expressions reported by Egüez et al, (2003) are triangular facets and shutter ridges which also represent the evidence for the latter dextral component of this segment.

Chingual Fault System

This segment follows across the Eastern Andean Cordillera and connects to La Sofia and Rio Cofanes Faults. Chingual system extends to Colombia and becomes the Afiladores-Subundoy-Algeciras Fault System. Its sense of movement corresponds to a dextral, strike-slip fault type. Morphological and geodetic evidences for right-lateral to compressional slip reveal are presented by Alvarado, (2012).

The average strike of this segment is N33°E (Egüez et al, 2003). Beauval et al, (2018) report that fault trace is 136 Km long and its depth and width is 18 Km. Average dip reported by the same authors reveals a vertical dipping angle to the NE.

Ego et al, (1996) proposes slip rate of 7 ± 3 mm/yr for this fault while closer to Colombian border Tibaldi et al, (2007) provides a range between 8.5 to 11. 4 mm/yr. Alvarado et al,

(2016) proposes this fault to be the major fault segment that accommodates the NAS migration to the NE.

METHODS

Location of tomographic sections

To select the tomographic section's location, we based in the geomorphic and structural descriptions carried out by different authors (see previous section) identifying geomorphological structures associated with fault tectonics along with the four segments of the CCPP fault. Figure 1 shows the location of tomography sections along the CCPP, to points were considered in each segment following the descriptions in Structural Context of CCPP section in order corroborate the geometric characteristics provided by these authors.

For Puná Segment one tomography section locates at Zambapala Ridge southeastern of Puná Island, this location has been intensively studied by Dumont et al, (2005) and the intra-continent tomographic section was selected near La Troncal town in the Gulf of Guayaquil considering descriptions carried out by Witt et al, (2005).

Pallatanga is the most studied segment. The work of Alvarado, (2012); Nocquet et al, (2014); Baize et al, (2014); Baize et al, (2020) characterizes extensively this segment. Our contribution to the knowledge of this fault structure will verify in subsurface the central (near Pallatanga) and northern (near Riobamba) sections, since these two segments are widely described in previous works.

Cosanga segment has less studies of its structure. We located the first tomographic section in Cosanga town, near Río Bermejo landslide, based in in the field observations of intense land-mass reptation in Cosanga town that could be associated to Cosanga Fault motion. The second tomographic section is located near Baeza town, based on structural descriptions

carried out in previous work of Egüez et al, (2003); Beauval et al, (2018).

For Chingual segment tomographic sections were selected based on Tibaldi et al,(2007) and Alvarado et al, (2016). First tomographic section was located near Río Cofanesand La Sofia fault since they are part of the Chingual Fault System. The secondtomographic section was located to the north, near La Bonita town.

Travel-time tomography

Travel-time observations allow us to obtain relevant information regarding the origin, the source that generates the seismic waves, and the speed at which the waves travel throughout the medium between the emitting source and the receivers. Travel-time tomography basis as described below according to Shearer, (2009).

Considering the path of a ray *s* through a medium whose velocity v varies with position; it is possible to express the travel-time T as:

$$T = \int \frac{1}{v(s)} ds = \quad \int u(s) ds \qquad (1)$$

This expression represents the integral of the inverse of velocity 1 / v (s) called slowness along the ray path. Now, if the slowness along various points in the ray path is disturbed by a differential variation of u, that is, δu (s), the travel time becomes:

$$T = \int \delta u(s) ds \qquad (2)$$

Thus, the travel time can be determined concerning the speed changes that caused them. It should be noted that δu (s) is small and does not affect the ray's path. To know the distribution of the slowness disturbance in the medium, it is necessary to study the ray's trajectories, which improves the resolution in the analysis. To do so, the previous expression can be discretized by dividing the medium into homogeneous blocks so that

the equation will become:

$$\Delta T_i = \sum_{j=1} G_{ij} \Delta u_j \qquad (3)$$

Where, G_{ij} is the distance that ray i travels in block j and Δu_j is the perturbation of slowness in block j.

Tomography sections

P velocity models were generated to obtain the tomography images in the points selected according to geomorphology along the CCPP mega-fault. The tomographic box was developed selecting the following six parameters.

1)   Extension of the tomographic box: lateral box extensions of 60 Km to appreciate local lithology and 120 Km were selected to infer geometric characteristics for the fault segments, respectively, (Figure 1).

2)   Depth: it was considered the thickness of the continental crust; since the study focuses only on active cortical faults, the vertical extension of the tomographic box was 45Km. The average thickness of the continental crust corresponds to 35 Km. Since the model begins approximately 5 km above the surface and at the same time the maximum altitude in Ecuador corresponding to the Chimborazo volcano was taken into account, 6.2 Km, 10 Km more have been added to the vertical extension of the tomographic section.

3)   Selection of seismic events: for the representativeness of seismic density necessary to obtain an accurate image of faults in-depth, we plotted all seismic events taking place in the first 20 Km on both sides perpendicularly to the tomographic section (Figure 1).

4)   Direction: all cuts at 60 Km of lateral extension considered an azimuth of N90°E

to have a better understanding of lithology and the 120 Km tomographic sections were generated considering strike followed by the mega-fault segments along the surface. To better appreciate the dipping angle of fault segments, we generated the tomographic sections perpendicularly to the fault-strike (Figure 1).

5) P-wave velocity models and interpretation: for this study, we use the P-wave relative velocity (%Vp). To obtain the relative velocity model, we make the difference between the *a posteriori* and the *a priori* models and then divided it into a priori flat layers model, being the result expressed in percentage. This model allows us to obtain a general image of underground changes in seismic P-wave velocity as indicators of regional crustal structures and fault segments' main geometry; it gives us more detailed and smaller-scale crustal structures. The velocity model anomalies and variations were associated with geological composition using Quaternary Faults data and geology maps for the studied zones and geomorphological structures appreciated in the surface.

6) Horizontal tomographic sections: horizontal cuts were carried out for the Cosanga segment to relate with geology. In this regard, we considered depth concerning the geoid with positive and negative depths representing tomographic cuts under and over the geoid, respectively.

RESULTS AND DISCUSSION

This study investigated the four segments of the CCPP fault, integrating the seismic data to infer their geometry in each segment and the surrounding stratigraphy.

Seismicity and travel-time tomography

Tomography sections were generated for each segment of the CCPP. The lateral extension and azimuth at which the tomographic sections were generated and locations selected can be appreciated in the following table:

Table 2: Location of tomographic sections presented in Figure 1 along CCPP fault segments.

Segment	Letter used in figures	Longitude	Latitude	Lateral extension	Azimuth
Puná	a	- 80.084	- 2.864		
Puná	b	- 79.629	- 2.625		
Pallatanga	c	- 78.980	- 2.045		
Pallatanga	d	- 78.756	- 1.665		
Cosanga	e	- 77.995	- 0.819	60 Km	N90°E
Cosanga	f	- 77.933	- 0.652		
Cosanga	g	- 77.853	- 0.450		
Chingual	h	- 77.688	0.299		
Chingual	i	- 77.608	0.414		
Puná	J	- 79.6916	- 2.6181		N148°E
Pallatanga	K	- 78.9883	- 2.0401	120 Km	N121°E
Cosanga	L	- 77.9907	- 0.6527		N110°E
Chingual	M	- 77.6419	0.36131		N127°E

Puná segment

Puná segment presents low seismic event density (Figure 6a) in Puná island. Meanwhile, there is a greater concentration of events (Figure 6b) located in the Coastal Region's continental crust, near the Gulf of Guayaquil and along the La Troncal Fault. This coastal fault system corresponds to the continental extension of the Puná segment that connects with the Pallatanga southernmost segment part of the CCPP fault system.

As can be appreciated in Figure 2, seismic activity concentrates mainly in the upper crust and shows negative values of ΔVp in the lowest range. This one indicates lower density materials corresponding to Holocene alluvial deposits (DGGM-IGM, 1979), which intensifies wave propagation differences. Puná segment corresponds to the southern limit of the NAS, and the subsidence dynamics of the Gulf of Guayaquil are attributed to the sliver's NE kinematic motion (Witt et al., 2005). Thus, the continental Puná segment (Figure 2b) would be related to NAS migration and consequent Gulf of Guayaquil

subsidence which would relate to the more intense density of seismic events in the intra-continent extension of Puná segment.
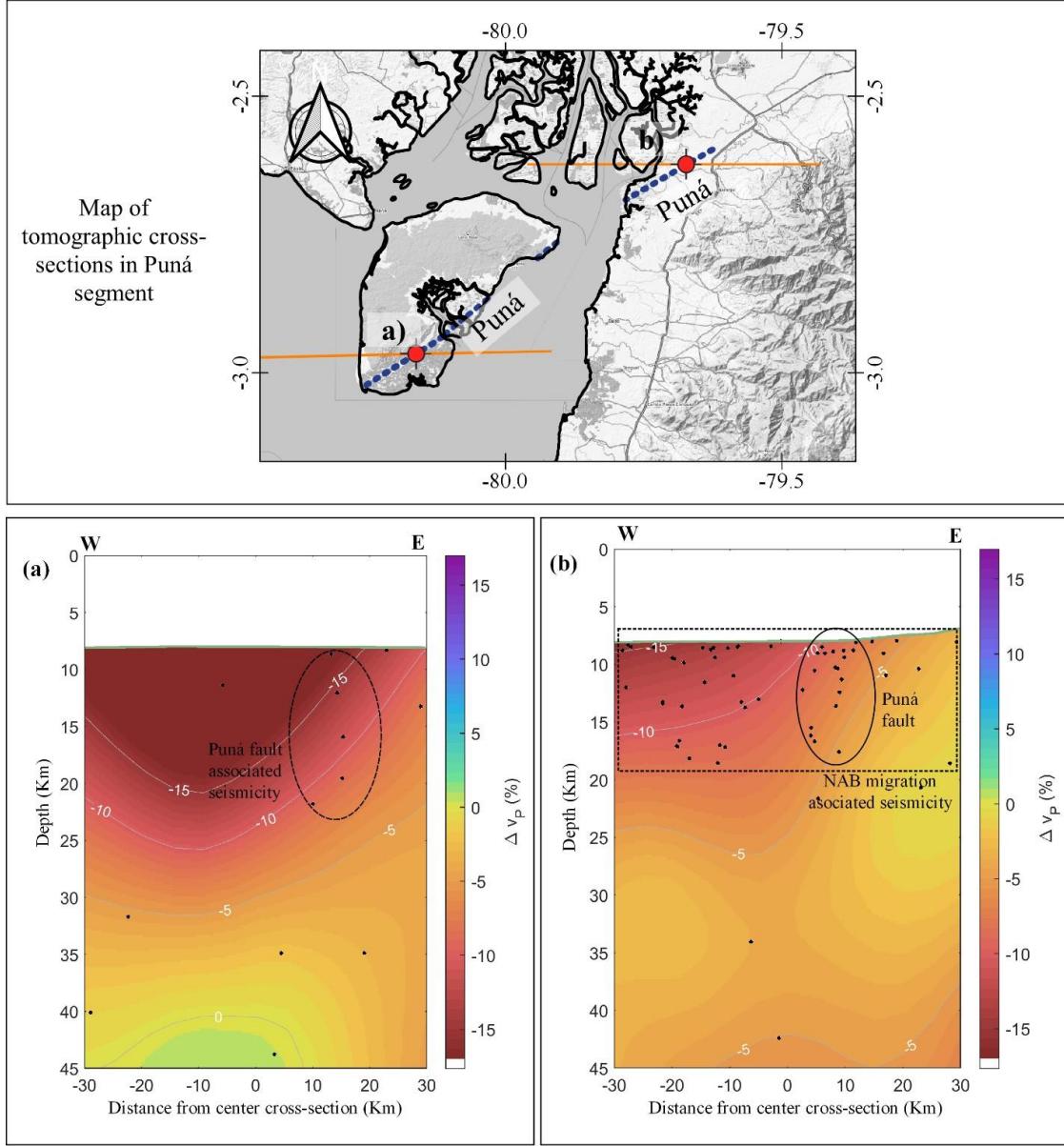

Figure 2. Tomographic cross-sections of Puná segment. The map shows the center of tomographic boxes (red dots) and the E-W box extension (orange lines). Puná fault is indicated in the map (blue dotted lines). Tomographic cross-sections were modeled using the parameter of variation of P-wave velocity, given in percentages (ΔVp.) (a) Isla Puná and (b) intra-continent continuation of Puná fault, in the Gulf of Guayaquil. Cross-

sections are N90°E. Black dots indicate seismic events recorded by RENSIG until 2016.

Pallatanga segment

In tomography sections for the Pallatanga segment, intense seismic activity can be appreciated. Figure 3a presents a cross-section of the southernmost segment of the

Pallatanga Fault, the solid ellipse indicates the alignment of seismic events. The fault runs 200 Km in NE direction to the Chimborazo volcano, extends more than 20 Km depth, and presenting a high dipping angle, as can be appreciated in figure 7a. These results are coherent with estimations by Beauval et al., (2018) of 18km deep inside the crust and 75° of dipping angle. Figure 3b cuts the northern section of Pallatanga fault. It shows a relatively vertical earthquake alignment deepening to 25 Km cutting the Sicalpa volcanic sediments,limited by Yunguilla and Robamba faults (DGGM-IGM, 1971). Beauval et al., (2018) estimates a 7.4mm/yr slip rate, which relates to the 7.1mm/yr of NAS slip rate reported by Alvarado et al., (2016). Figure 3b also shows intense seismic activity to the furthest right of the tomography cross-section. This intense activity can be attributed to volcanic seismicity from the Tungurahua volcano approximately 15 Km to the north.
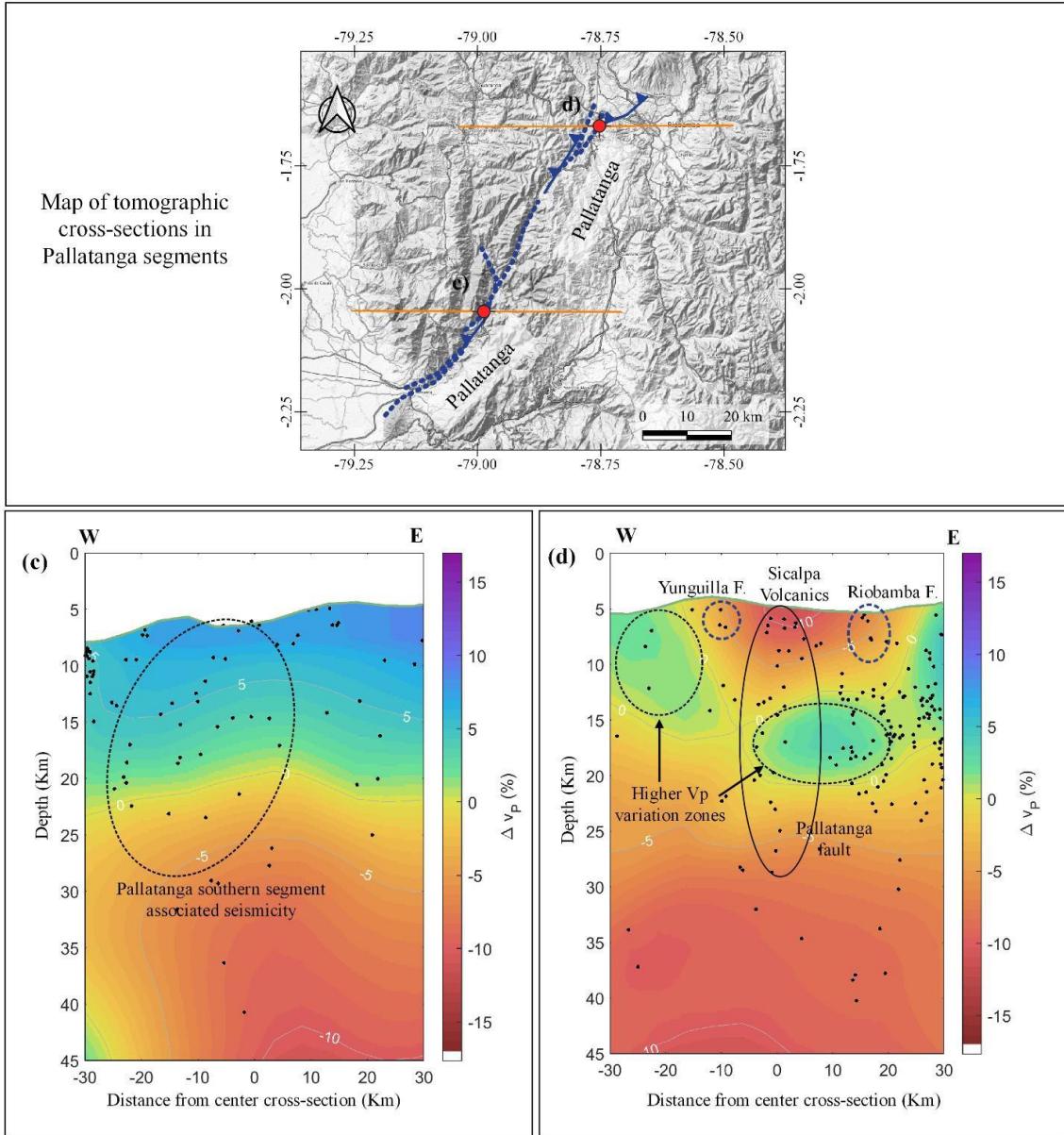
Figure 3. Tomographic cross-sections of Pallatanga segment. The map shows the center of tomographic boxes (red dots) and the E-W box extension (orange lines). Pallatanga segments are indicated in the map (blue dotted lines). Tomographic cross-sections were modeled using the parameter of variation of P-wave velocity, given in percentages (ΔVp.) (c) near Pallatanga town cross-section and (d) near Riobamba city cross-section. Tomographic cross-sections are oriented N90°E. Black dots indicate seismic events recorded by RENSIG until 2016.

Cosanga Segment

Figure 4 shows seismic events for the Cosanga segment, which comprises severalreverse faults that conform to this section of the CCPP. Figures 4e and 4f present seismicevents concentration approximately 20 Km in depth and coincides with a change in ΔVp values. These events might result from the compressive effect of energy liberation from block interaction between hanging and footwalls in reverse faults such as the Cosanga segment.

Figure 4g ΔVp model near Baeza town shows a clear difference between two different types of lithologies. One to the left presents positive values of ΔVp. Tomography cross-section, in this case, might be marking the limit between sedimentaryrocks of Margajitas Group to the left and basaltic lavas from Sumaco volcanic to the right(DGGM-IGM, 1986), which are covered by alluvial deposit strata. In this segment of theCCPP fault system dipping angles are differ from the almost vertical dipping angles appreciated in Figures 2 and 3, turning to a NW dipping as described by Egüez, et al (2003), and coherent with the values reported by Tibaldi, et al (2007) of ~70°.
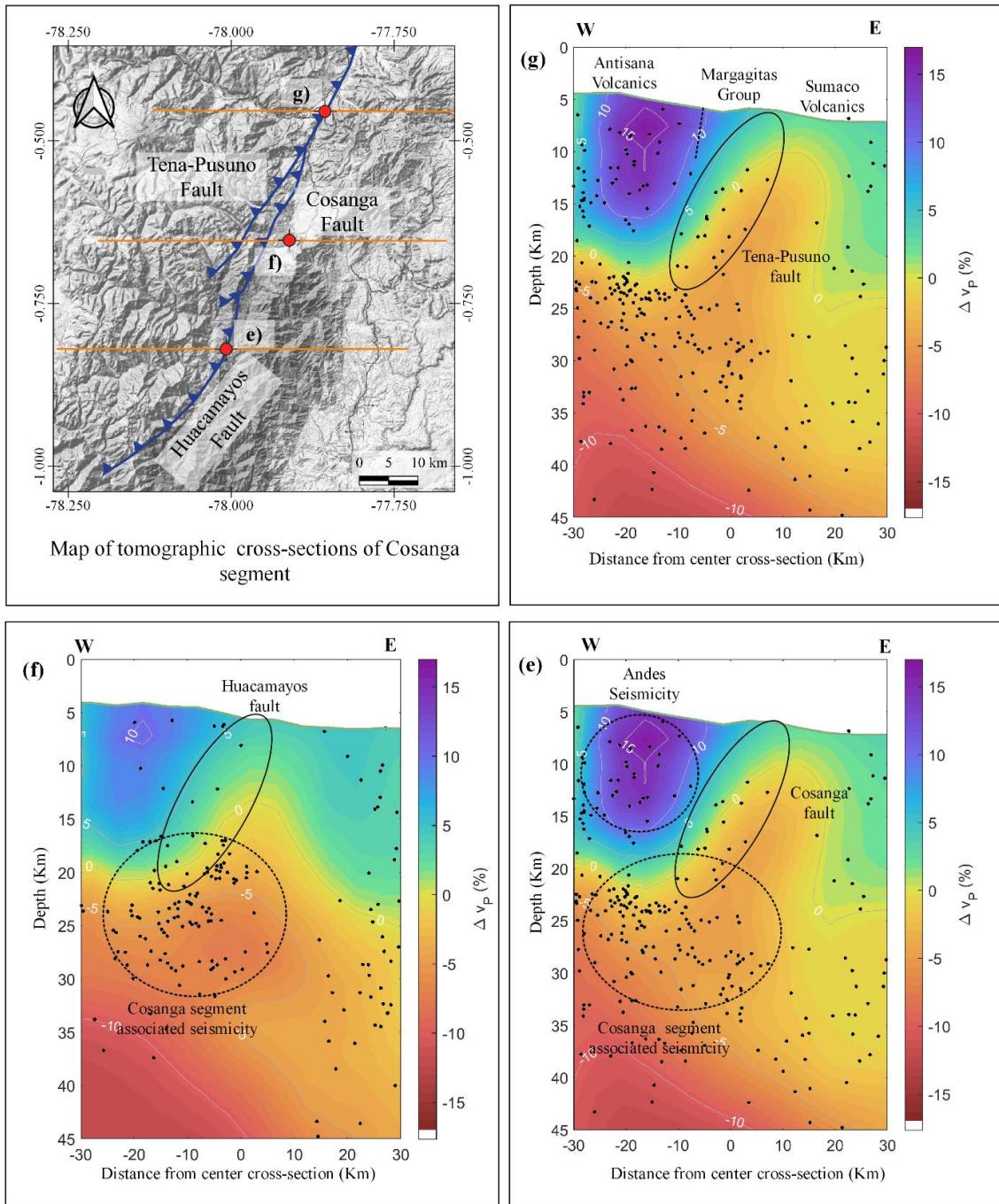
*Figure 4. Tomographic cross-sections of Cosanga segment. The map shows the center of tomographic boxes (red dots) and the E-W box extension (orange lines). Cosanga segments are indicated in the map (blue saw-teethed lines). Tomographic cross-sections were modeled using the parameter of variation of P-wave velocity, given in percentages (ΔVp.) (e) Huacamayos Fault cross-section, (f) Cosanga town cross-section and (g) near*

Figure 5 shows a horizontal cut for the Cosanga segment at -1.0 Km depth to the geoid. This tomographic section can identify a *ΔVp* discontinuity between 3 and 3.5%, which represents the trace of the fault and the limit between meta-volcanic Cretaceous lithology from Llanganates Group and lahar deposits associated to Sumaco and Pan de Azúcar volcanic edifices. (DGGM-IGM, 1986). Río Bermejo landslide locates at the convergence of two reverse faultsthat comprise the Cosanga Fault System, part of the CCPP,Tena-Pusuno and Cosanga Faults.
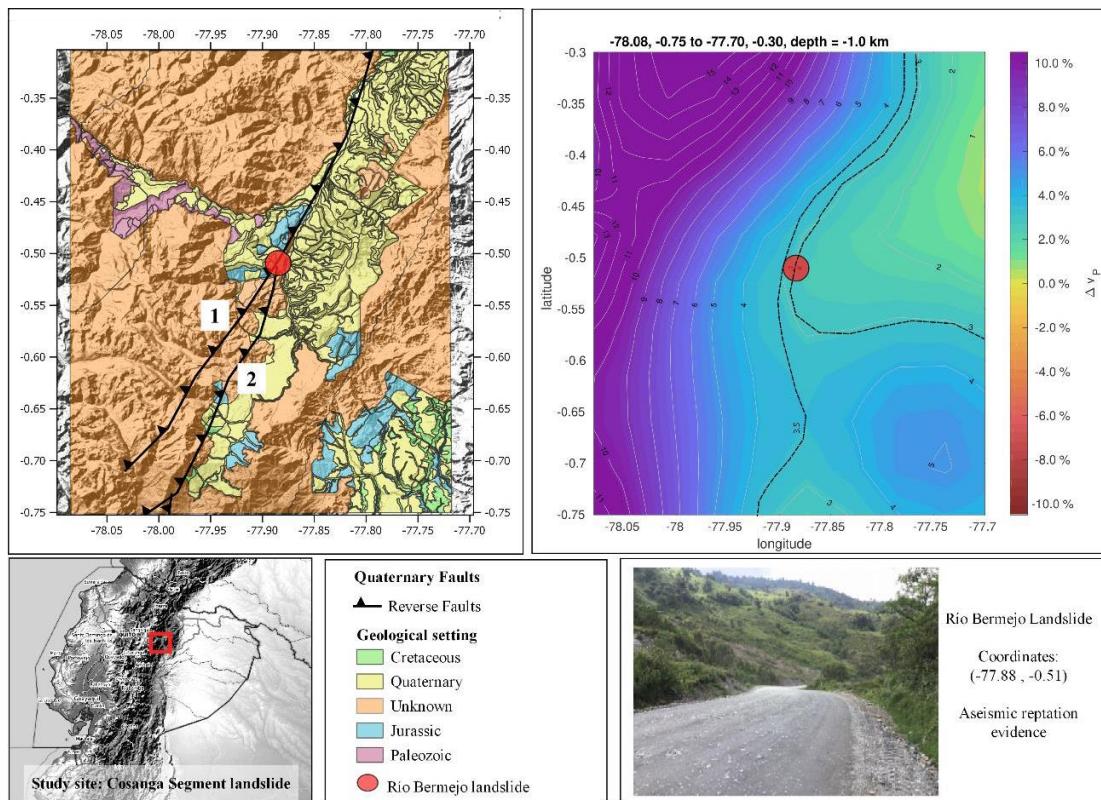
Figure 5. Geological setting of the Cosanga fault segment (upper left) with reverse faults Tena-Pusuno (1) and Cosanga (2). The horizontal tomographic section for the Cosanga Segment (upper right), using Vp-wave variation (%). Río Bermejo mass movement position plotted with a red circle locates in the geologic map in the contact of two reverse

faults, Huacamayos and Cosanga Faults which coincides with a change in the ΔVp in the

horizontal cross-section (upper right map).

Chingual segment

Chingual tomographic sections show a very low density of earthquake events. Besides the 1834 Subundoy area earthquake (magnitude 7.4), no considerable activity is registered for this segment in the present time (Yepes et al., 2016). Seismic activity appears to be shallow in the northern section of the fault, having very few events located between seven and eighteen kilometers in depth. As can be appreciated from the earthquake's alignment in Figure 6 Chingual segment extends with an azimuth of approximately N30°E. The strike coincides with Eguez et al., (2003) analysis for this fault segment. Seismic events deepen in the southern section of the fault, reaching more intense activity down to 20 Km. This increase in activity might be attributed to the Chingual segment's connection to the Cosanga segment to the south, (Yepes et al., 2016). To the north Chingual segment connects with Afiladores-Subundoy-Algeciras faults system in Colombia (Paris et al., 2000).

Tomography sections for the Chingual segment are shown in Figures 6a and 6b. In both tomography boxes, Chingual fault marks the limit between Cordillera Real metamorphic rocks such as the Rosa Florida batholith and the quartzite and gneiss rocks from Cofanes Group (DGGM-IGM, 1973) and lateral variation of ΔVp differentiates Napo Formation sedimentary rocks.
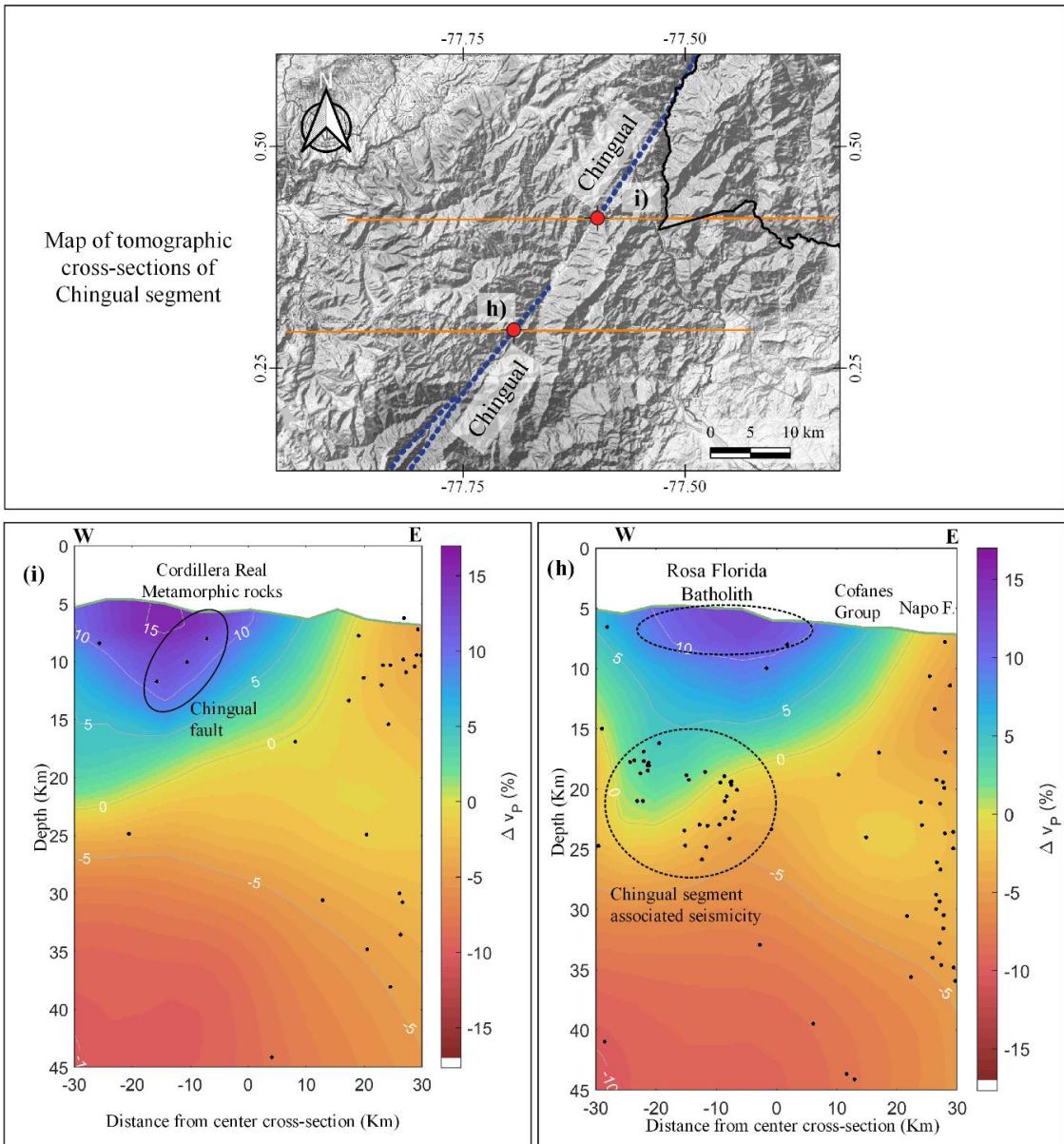
Figure 6. Tomographic cross-sections of Chingual segment. The map shows the center of tomographic boxes (red dots) and the E-W box extension (orange lines). Chingual segments are indicated in the map (blue dotted lines). Tomographic cross-sections were modeled using the parameter of variation of P-wave velocity, given in percentages (ΔVp). (h) near La Sofia cross-section, (i) near La Bonita cross-section. Tomographic cross-sections are oriented N90°E.

CCPP fault geometry

In order to identify the fault geometry, tomographic sections were generated considering the P-wave velocity variation model. It gives us a better understanding of the local characteristic's depth. One cut was considered for every segment, each one had a 120 Km horizontal extension, and seismic references were located for each cut.

For Puná segment Figure 7J, the tomographic cross-section was located in the continental crust since there is more intense seismicity along this section of the fault tracethan in Puná Island itself. It is necessary to place the tomographic plots in zones where seismicity can give clues of fault geometry. This section of the Puná fault shows an intense concentration of shallow seismicity with sparse events that give a width of approximately 20 Km and a vertical dipping angle; they determined the same values usinggeologic and geodetic models. Seismicity in this section stops at about 20 Km, consistent with the value reported by Beauval et al., (2018). Earthquakes mark an eastern limit for anegative value of ΔVp, indicating more homogenous geologic material extending to 23 Km in depth.

Pallatanga segment comprehends three sections northern, center, and southern fault traces. As shown in Figure 7K, there is shallow yet intense seismicity in this zone. Events describe a marked vertical (90°) dipping defining the eastern limit between two materials with a $\Delta Vp$of 5% and 0%, respectively. Egüez et al., (2003) describe the fault orientation as an approximate N18°E strike and an unknown dipping angle in the West direction. (Egüez et al., 2003; Beauval et al., 2018) report a dipping angle of 75° for northern segment of Pallatanga fault. We appreciate the vertical dipping angle (90°) of thesouthern section in the tomographic cross-section. Events seem to concentrate on the first15 Km crust for this tomographic section. Since seismic events are very concentrated, fault

width appears to be approximately 15 Km. Beauval et al., (2018) reports similar values for Pallatanga fault geometry, 18 and 19 Km respectively.

Cosanga segment (Figure 7L) tomographic image reveals intense seismicitydeeper from 20 to 30 Km and the most superficial events also mark a limit between materials with different velocity variation. Cosanga fault shows a reverse dynamic of motion, and its dipping angle can clearly define it. Egüez et al., (2003) report an unknowndipping angle oriented to the NW whilst the tomographic cross-section generated in this study, shows a dipping angle of approximately 78°, which relates to the value reported byTibaldi et al., (2007) of ~70°. Cosanga segment comprises the following reverse faults: Tena-Pusuno, Cosanga and Huacamayos. The present study located the cross-section in the convergence point between the Tena-Pusuno fault system and Baeza-Chaco faults. There is also a considerable variation of width, with narrow extension in the first kilometers and expanding to nearly 40 Km in the deepest part of the fault, similarly to Beauval et al.,(2018) that reports a fault trace of 36 Km deep. Also, as can be appreciated in Figure 4 greater concentration of seismic events locates from 20 to 30 Km deep.

In Figure 7M that represents Chingual fault it is possible to identify an almost vertical dipping (82°). This value differs slightly from Beauval et al, (2018) and Egüez et al., (2003) that reported a 90° dipping angle, probably due to different methodologies in the assessment of this value, while this study uses seismic data, Beauval et al, (2018) andEgüez et al., (2003) use geodetic models and photo-interpretation respectively. The shallowest seismic events are located within the limit of velocity variations. El Ángel faultto the left and an unknown fault to the right side mark the limit of a considerable differenceof p-wave velocity, where the shallower events of Chingual fault are located. Seismicity ends at approximately 12 Km to reappears at 25 Km. According to Beauval et al., (2018), Chingual segment depth extends to 18 Km coinciding with the density of events forming

Chingual segment (Figure 7M). Also, seismic events location show a width of approximately 20 Km from the shallowest to the deepest part of the fault. These results are coherent with those reported by Beauval et al, (2018).
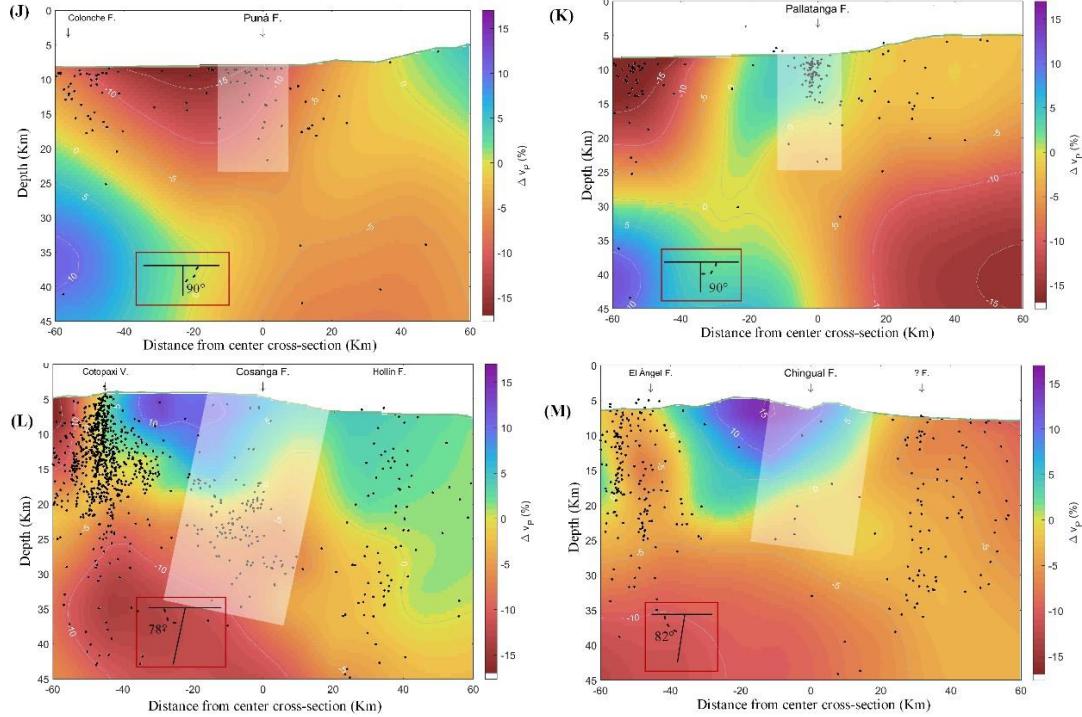

Figure 7. Tomographic sections of the CCPP mega-fault, tomographic model represents variation of p-wave velocity model, measured in %. Puná segment (J) oriented N148°E, Pallatanga segment (K) oriented N121°E, Cosanga segment (L) oriented N110°E and Chingual segment (M) oriented N127°E. White rectangle indicates seismic events associated to the fault segments considered to infer depth and width. Botton left angles indicate dipping angles of each segment.

CONCLUSIONS

This study presents in-depth crustal imaging for the CCPP mega-fault and associates it with the lithology of its segments to deliver a comprehensive interpretation of this fault system geometry and seismicity.

In the ΔVp model, the low density of seismic events is appreciated outside the continental crust. Seismicity increases entering the Gulf of Guayaquil where the trace connects to the Pallatanga segment.

It connects to the Puná segment, cross-cutting the Western Cordillera it runs along the Interandean valley. The fault has a southern, central, and northern segment. It has an almost vertical dipping angle and extends more than 20 Km deep in the crust.

ΔVp model near Baeza town shows a clear difference between two different types of lithologies. The reverse fault increases seismic events considerably between 20-30 Km and a dipping angle of 78°, which differs from values reported in past studies.

The location of the Río Bermejo landslide coincides with a change in the horizontal tomographic section of Cosanga segment. It reveals a discontinuity in ΔVp model between 2 and 3% at which two reverse faults (Tena-Pususno Fault and Cosanga Fault) converge.

Lateral variation of ΔVp differentiates Napo Formation sedimentary rocks from batholitic structures. Tomographic cross-sections also reveal a high dipping angle of about 82° to the west.

REFERENCES

Alvarado, A. (2009). Falla Pallatanga, in Atlas de deformaciones cuaternarias de los Andes. Servicio Nacional de Geología y Minería, Publicación Geológica Multinacional, No.7, 288-293.

Alvarado, A. (2012). Néotectonique et cinématique de la déformation continentale en Equateur. Sciences de la Terre. Université de Grenoble, 2012. Français. NNT : 2012GRENU026.

Alvarado, A., Audin, L., Nocquet, J. M., Jaillard, E., Mothes, P., Jarrín, P., Segovia,

M., Rolandone, F. & Cisneros, D. (2016). Partitioning of oblique convergence in the Northern Andes subduction zone: Migration history and the present-day boundary of the North Andean Sliver in Ecuador. Tectonics, 35(5), 1048-1065.

Araujo, S. (2016). Travel time tomography of the crust and the mantle beneath Ecuadorfrom data of the national seismic network (Doctoral dissertation, Université Grenoble Alpes (ComUE)).

Araujo, S., Troncoso, L., & Ruiz, M. (2009). Relocalización por dobles diferencias del clúster sísmico de Pisayambo. La Granja.

Aspden, J. A., & Litherland, M. (1992). The geology and Mesozoic collisional history of the Cordillera Real, Ecuador. *Tectonophysics*, *205*(1–3), 187–204.

Baize, S., Audin, L., Winter, T., Alvarado, A., Moreno, L. P., Taipe, M., Reyes, P., Kauffmann, P. & Yepes, H. (2014). Paleoseismology and tectonic geomorphology of the Pallatanga fault (Central Ecuador), a major structure of the South-American crust. Geomorphology, 237, 14-28.

Baize S, Audin L, Alvarado A, Jomard H, Bablon M, Champenois J, Espin P, SamaniegoP, Quidelleur Xand Le Pennec J-L (2020) ActiveTectonics and Earthquake GeologyAlong the Pallatanga Fault, Central Andes of Ecuador. Frontiers on Earth Science. 8:193.

Beauval, C., Yepes, H., Palacios, P., Segovia, M., Alvarado, A., Font, Y., Aguilar, J., Troncoso, L. & Vaca, S. (2013). An earthquake catalog for seismic hazard assessment in Ecuador. Bulletin of the Seismological Society of America, 103(2A), 773-786.

Beauval, C.; Marinière, J.; Yepes, H.; Audin, L.; Nocquet, J.-M.; Alvarado, A.; Baize,S.;

Aguilar, J.; Singaucho, J.-C.; Jomard, H. (2018). A New Seismic Hazard Model for Ecuador. Bulletin of the Seismological Society of America, 108(3A),1443–1464. doi:10.1785/0120170259

Bilek, S. L. (2010). Seismicity along the South American subduction zone: Review oflarge earthquakes, tsunamis, and subduction zone complexity. *Tectonophysics*, *495*(1–2), 2–14.

Deniaud, Y., Baby, P., Basile, C., Ordoñez, M., Montenegro, G., & Mascle, G. (1999). Opening and tectonic and sedimentary evolution of the Gulf of Guayaquil: Neogene and Quaternary fore-arc basin of the south Ecuadorian Andes. ComptesRendus de l'Academie des Sciences Series IIA Earth and Planetary Science, 3(328), 181-187.

Diederix, H., Audemard, F., Osorio, J. A., Montes, N., Velandia, F., & Romero, J. (2006). Modelado morfotectónico de la falla transcurrente de Ibagué, Colombia.Revista de la Asociación Geológica Argentina, 61(4), 492-503.

DGGM-IGM, (1971). Mapa Geológico del Ecuador. Riobamba. Hoja CT-MIV-E, 3888, escala 1:100 000. Quito. Dirección General de Geología y Minas - Instituto Geográfico Militar, 1 map with text.

DGGM-IGM, (1973). Mapa Geológico del Ecuador. Isla Puná. Hoja CT-MV-F, 3585, escala 1:100 000. Quito. Dirección General de Geología y Minas - Instituto Geográfico Militar, 1 map with text.

DGGM-IGM, (1979). Mapa Geológico del Ecuador. Bucay. Hoja CT-NV-B, 3585,escala 1:100 000. Quito. Dirección General de Geología y Minas - Instituto Geográfico Militar, 1 map with text.

DGGM-IGM, (1981). Mapa Geológico del Ecuador. San Gabriel. Hoja CT-OII-C, 4095,

escala 1:100 000. Quito. Dirección General de Geología y Minas – Instituto Geográfico Militar, 1 map with text.

DGGM-IGM, (1986). Mapa Geológico del Ecuador. Baeza. Hoja CC-OIII-C, 4092,escala 1:100 000. Quito. Dirección General de Geología y Minas - Instituto Geográfico Militar, 1 map with text.

DGGM-IGM, (1987). Mapa Geológico del Ecuador. Mariano Acosta. Hoja CT-OII-D, 4094, escala 1:100 000. Quito. Dirección General de Geología y Minas - Instituto Geográfico Militar, 1 map with text.

Dumont, J. F., Santana, E., & Vilema, W. (2005). Morphologic evidence of active motion of the Zambapala Fault, Gulf of Guayaquil (Ecuador). *Geomorphology*, *65*(3–4), 223–239.

Eguez, A., Alvarado, A., Yepes, H., Machette, M. N., Costa, C., Dart, R. L., & Bradley, L. A. (2003). Database and map of Quaternary faults and folds of Ecuador and its offshore regions. US Geological Survey Open-File Report, 3, 289.

Lonsdale, P. (1978). Ecuadorian subduction system. AAPG Bulletin, 62(12), 2454-2477.

Nocquet, J., Villegas-Lanza, J., Chlieh, M., Mothes, P., Rolandone, F., Jarrin, P., Cisneros, D., Alvarado, A., Audin, L., Bondoux, F., Martin, X., Font, Y., Régnier,M., Vallée, M., Tran, T., Beauval, C., Maguiña Mendoza, J., Martinez, W., Tavera, H. & Yepes, H. (2014). Motion of continental slivers and creeping subduction in the northern Andes. Nature Geoscience, 7(4), 287–291.

Paredes, C. D., & Araujo, S. (2021). The use of seismic tomography to describe theupper crustal structure beneath the Chalupas Caldera, Ecuador. *REM - International Engineering Journal*, *74*(2), 189–197.

Palacios Lopez, W. (1983). Estudio Geológico de la Parte Nororiental de la Isla Puna (Bachelor's thesis, Espol).

Paris, G., Machette, M.N., Dart, R.L., and Haller, K.M. (2000). Map and database of Quaternary faults and folds in Colombia and its offshore regions: USGS Open-File Report 00-0284, 60 p.

Pastén-Araya, F., Potin, B., Ruiz, S., Zerbst, L., Aden-Antonióv, F., Azúa, K., Rivera,E., Rietbrock, A., Salazar, P., & Fuenzalida, A. (2021). Seismicity in the upper plate of the Northern Chilean offshore forearc: Evidence of splay fault south of the Mejillones Peninsula. *Tectonophysics*, *800*, 228706.

Pratt, W. T., Duque, P., & Ponce, M. (2005). An autochthonous geological model for the eastern Andes of Ecuador. *Tectonophysics*, *399*(1-4 SPEC. ISS.), 251–278.

Shearer, P. (2009). Introduction to Seismology Second Edition. In *Cambridge University Press: Vol. (5)2* (Second Edition, Issue 2).

Tibaldi, A., Rovida, A., & Corazzato, C. (2007). Late Quaternary kinematics, slip-rate and segmentation of a major Cordillera-parallel transcurrent fault: The Cayambe-Afiladores-Sibundoy system, NW South America. *Journal of Structural Geology*, *29*(4), 664–680.

Velandia, F., Acosta, J., Terraza, R., & Villegas, H. (2005). The current tectonic motion of the Northern Andes along the Algeciras Fault System in SW Colombia. *Tectonophysics*, *399*(1-4 SPEC. ISS.), 313–329.

Witt, C., Bourgois, J., Michaud, F., Ordoñez, M., Jiménez, N., & Sosson, M. (2006). Development of the Golfo de Guayaquil (Ecuador) as an effect of the North Andean block tectonic escape since the Lower Pleistocene. Tectonics, 25, TC3017.

Yepes, H., Audin, L., Alvarado, A., Beauval, C., Aguilar, J., Font, Y., & Cotton, F. (2016). A new view for the geodynamics of Ecuador: Implication in seismogenic source definition and seismic hazard assessment. Tectonics, 35(5), 1249-1279.